Available online at www.sciencedirect.com
ScienceDirect
Planetary and Space Science 55 (2007) 631–642
Planetary and Space Science
www.elsevier.com/locate/pss

Mass loss of "Hot Jupiters"—Implications for CoRoT discoveries. Part I: The importance of magnetospheric protection of a planet against ion loss caused by coronal mass ejections

M.L. Khodachenko[a,*], H. Lammer[a], H.I.M. Lichtenegger[a], D. Langmayr[a], N.V. Erkaev[b], J-M. Grießmeier[c,d], M. Leitner[a], T. Penz[a], H.K. Biernat[a], U. Motschmann[d], H.O. Rucker[a]

[a]*Space Research Institute, Austrian Academy of Sciences, Schmiedlstr. 6, A-8042 Graz, Austria*
[b]*Institute for Computational Modelling, Russian Academy of Sciences, 660036 Krasnoyarsk-36, Russian Federation*
[c]*LESIA, CNRS-Observatoire de Paris, 92195 Meudon, France*
[d]*Institut für Theoretische Physik, Technische Universität Braunschweig, Mendelssohnstrasse 3, D-38106 Braunschweig, Germany*

Received 13 January 2006; accepted 5 July 2006
Available online 2 November 2006

Abstract

Atmospheric erosion due to CME-caused ion pick-up is investigated here for the first time for short periodic gas giants (so-called "Hot Jupiters") orbiting close to a star. To study the effect of encountering CMEs produced on the magnetospheres and atmospheres of "Hot Jupiters" we model possible interaction of dense CME plasma with the exoplanet HD209458b ($r_{pl} = 1.43 r_{Jup}$, $M_{pl} = 0.69 M_{Jup}$), which orbits a 4.0–5.0 Gyr old Sun-like star at a distance of about 0.045 AU. A numerical hydrodynamic model is applied for calculation of the upper atmospheric density and the hydrogen wind of HD209458b as a function of planetocentric distance. Taking into account the similarity of HD209458b's host star to our Sun we use for the study of the ion production and loss rate of H^+ ions the solar CME plasma parameters and apply a numerical test particle model. Tidal-locking of short periodic exoplanets closely located to their host stars should result in weaker intrinsic planetary magnetic moments, as compared to those of the fast rotating Jupiter type planets at much larger orbits. It is shown that in this case the encountering CME plasma can compress the magnetospheric stand-off distance of short periodic "Hot Jupiters" down to the heights at which the ionization and pick-up of the planetary neutral atmosphere by the CME plasma flow take place. Assuming for the host star of HD209458b the same CME occurrence rate as on the Sun, we estimate possible total mass loss rates of HD209458b due to its collisions with CMEs over the planet lifetime. It has been found that under different estimations of the value of a planetary magnetic moment, HD209458b could have lost over its lifetime the mass from 0.2 up to several times of its present mass M_{pl}.

Keywords: Hot Jupiters; CMEs; Stellar winds; Magnetosphere and atmosphere interaction with CME plasma; Ion loss; CoRoT

1. Introduction

The present (status May, 2006) number of 188 discovered exoplanets[1] will be largely enhanced after the launch of the CoRoT space observatory in 2006, which will use high precision photometry for detection of planetary transits. Applying known statistics of discovered "Hot Jupiters" to the planned 1.8×10^5 light curves obtained during the CoRoT mission, one can expect the discovery of about 200 additional short-periodic gas giants with masses $\geqslant 0.1 M_{Jup}$ and orbital periods <10 days (Moutou et al., 2003). As pointed out by Baraffe et al. (2004) and Langmayr et al. (2006) one of the aims of the study of discovered "Hot Jupiters" is a better understanding of the evolution of their mass–radius relation over their history. For this purpose it is important to understand all possible thermal and non-thermal atmospheric loss processes of "Hot Jupiters" over their evolutionary time scales.

*Corresponding author. Tel.: +43 316 4120661; fax: +43 316 4120690.
E-mail address: maxim.khodachenko@oeaw.ac.at (M.L. Khodachenko).
[1]http://exoplanet.eu/index.php

0032-0633/$ - see front matter © 2006 Elsevier Ltd. All rights reserved.
doi:10.1016/j.pss.2006.07.010

Vidal-Madjar et al. (2003) observed with the Hubble Space Telescope Imaging Spectrograph (HSTIS) an evaporating hydrogen-rich atmosphere corresponding to a mass loss rate $>10^{10}\,g\,s^{-1}$ around the short periodic gas giant HD209458b. Follow-up observations by Vidal-Madjar et al. (2004) detected also O and C atoms up to the Roche lobe at about $2.5r_{pl}$, indicating that these heavy species must be carried up to this distance and beyond most likely in a state of hydrodynamic "blow-off" (Lammer et al., 2003a; Vidal-Madjar et al., 2004; Lecavelier-des-Etangs et al., 2004; Baraffe et al., 2004; Yelle, 2004; Tian et al., 2005; Langmayr et al., 2006).

Recent photochemical calculations by Yelle (2004) of the thermospheric structure of giant exoplanets in orbits with semi-major axes from 0.01–0.1 AU are in agreement with the study by Lammer et al. (2003a) who have shown that the upper atmospheres of these short periodic hydrogen-rich gas giants can be heated to more than 10 000 K by the high X-ray and extreme ultraviolet (XUV) flux from the central star. These high temperatures cause the neutral atmosphere to expand and escape rapidly. During such an expansion, the upper thermosphere is cooled by high escape rates (Yelle, 2004; Tian et al., 2005; Langmayr et al., 2006), while the lower thermosphere is cooled primarily by radiative emissions from molecular H_3^+ ions, created by photoionization of H_2 and subsequent ion chemistry (Yelle, 2004).

The growing evidence that such hydrogen-rich "Hot Jupiters" experience a hydrodynamic atmospheric "blow-off" gives reason to consider that their planetary winds may directly interact with the incoming stellar plasma flows (Grießmeier et al., 2004; Erkaev et al., 2005). Grießmeier et al. (2004) modelled the stellar wind interaction with short periodic gas giants for the present and for early evolutionary stages of solar-like stars. They found that it may be possible that short periodic gas giants can have an ionosphere–stellar wind interaction similar to that one on Venus, because the internal magnetic moments of such exoplanets orbiting close to their host stars are expected to be weaker compared to Jupiter due to their tidal locking. Grießmeier et al. (2004) estimated that the magnetic moments of tidally locked "Hot Jupiters" at orbital distances of about 0.045 AU can be $\leqslant 0.1\mathscr{M}_{Jup}$, where $\mathscr{M}_{Jup}$ is the present time value of the magnetic moment of Jupiter orbiting the Sun at 5 AU. In such a case, evaporating upper neutral atmospheres of exoplanets which are unprotected or weakly protected by their small magnetospheres will be affected by the dense stellar plasma flow and by non-thermal ion loss processes.

Interaction of short-periodic exoplanets with the stellar wind plasma and high XUV flux at close orbital distances plays a crucial role regarding the ionization and ion loss processes of atmospheric species. Erkaev et al. (2005) showed that short-periodic gas giants, similar to HD209458b, at orbital distances <0.1–0.2 AU around solar-like G-type stars with ages comparable to our Sun, may have stellar wind induced H^+ ion loss rates in the orders of about 10^8–$10^9\,g\,s^{-1}$, which are lower than the observation-based and modelled neutral hydrogen loss rates of about 10^{10}–$10^{12}\,g\,s^{-1}$ (Lammer et al., 2003a; Vidal-Madjar et al., 2004; Lecavelier-des-Etangs et al., 2004; Baraffe et al., 2004; Yelle, 2004; Tian et al., 2005; Langmayr et al., 2006). In that respect, the interaction of these exoplanets with stellar coronal mass ejections (CMEs) appears to be an important process, which is essential for a better understanding of the mass loss on "Hot Jupiters". CMEs are large-scale magnetized plasma clouds carrying billions of tons of material that erupt from the star and propagate in the stellar heliosphere, interacting in multiple ways with the stellar wind. High speed, intrinsic magnetic field and the increased density as compared to the stellar wind background make CMEs an active factor which strongly influences the planetary environments and magnetospheres. Due to the close distance to their host stars, "Hot Jupiters" should relatively often experience collisions with the CMEs plasma. During these collisions the planetary magnetospheres may be compressed much deeper inside the atmosphere towards the visible radius of the exoplanet. This would result in much higher ion loss rates than during usual stellar wind conditions.

To compare the ion loss triggered by CMEs, which collide with "Hot Jupiters", to the ion loss rates under usual stellar wind conditions as estimated by Erkaev et al. (2005), we focus in this study on the expected CME–magnetosphere–atmosphere interaction, by using the observations-based knowledge about CMEs on the Sun. As an example we study the interaction of the CME plasma with the well observed short periodic gas giant HD209458b, which orbits a 4.0–5.0 Gyr old Sun-like G-type star at 0.045 AU (e.g., Barman et al., 2002; Vidal-Madjar et al., 2003). By this, a circular orbit of the planet is assumed. This assumption is quite reasonable as HD209458b is known to have an eccentricity of about 0.07 (http://exoplanet.eu/catalog-all.php).

Based on Ca II H & K activity measurements during 4 years (from 11.6.1999 to 15.7.2003), Wright et al. (2004) determined for the host star HD209458 the mean value of its Mount Wilson activity index $S = 0.154$ (with a standard error of 1.4%), and calculated the true chromospheric activity index value $\log(R'_{HK})$ as well as the rotation period, which appeared to be -5 and 19 days, respectively. Note that the present time Sun has S-values between 0.167 and 0.179 (for the cycle minimum and maximum, respectively) and the solar $\log(R'_{HK})$ (Noyes et al., 1984) value is -4.93 (for $S = 0.171$). Therefore, HD209458 has a comparable activity level to the present day Sun, and the application of solar CMEs parameters in our study may in this particular case be justified by this similarity.

Of course, due to the relatively short (4 years) monitoring time of HD209458 (Wright et al., 2004) it is difficult to judge about an activity cycle of this star, which is probably longer. It is also impossible to say whether the star has been in minimum, maximum, or middle activity phase during these 4 years. At the same time, since in our study we are

interested in rather long time periods, all cycle variations as well as possible short-time depletions of the stellar activity like Maunder minimum seem not to produce strong effect, as they are averaged on the planetary evolution time scales.

In Section 2 we summarize the main physical characteristics of solar CMEs and estimate the maximum and minimum number density and velocity of solar CMEs as a function of their orbital distance. We provide an observation-based interpolation of this dependence, which is used further for modelling of the CME-caused atmospheric erosion of HD209458b.

In Section 3 we discuss the extrapolation of solar CME plasma parameters to extra-solar CMEs and estimate roughly the expected frequency of CME collisions with the exoplanet.

In Section 4 we study the minimum and maximum expected efficiency of the CME plasma interaction with the magnetosphere and atmosphere of HD209458b. For the calculation of the atmospheric ion pick-up loss rates we use the numerical test particle model which includes the effects of ionization by the CME plasma (charge exchange, electron impact) and XUV radiation. The model is applied to the upper neutral atmosphere and the hydrogen wind, which is calculated by a hydrodynamic model (see Langmayr et al., 2006). Further, we compare the results with the estimated stellar wind ion pick-up loss rates under usual stellar activity conditions (Erkaev et al., 2005). Since, the appearance of CMEs is connected with the stellar activity period over evolutionary time scales, we estimate in Section 5 the expected total mass loss rates of HD209458b over its history and discuss the implications of our findings for the expected discoveries of "Hot Jupiters" during the CoRoT mission.

2. General features of CME activity

The current knowledge on CMEs comes from the study of the Sun. Significant impact on this study has been made by the large angle and spectrometric coronagraph (LASCO) on board of ESA Solar and Heliospheric Observatory (SoHO), which observed more than 8000 CMEs since January 1996. Due to the existence of two spatial domains of observations, the term CME is usually applied for ejecta as they are observed near the Sun ($\leqslant 0.14$ AU), whereas at the larger distances they are traditionally called interplanetary CMEs (ICMEs). Solar CMEs and ICMEs are well described in the literature (Gopalswamy, 2003, 2004; St. Cyr et al., 2000) and here we just briefly summarize their main features, which make them an important planetary affecting factor.

2.1. CME origin, relation to flares and global structure

CMEs are associated with flares and prominence eruptions and their sources are usually located in active regions and prominence sites. Closed magnetic structure is the basic characteristic of CME producing regions. Recent studies on temporal correspondence between CMEs and flares provide arguments in favor of the so-called common-cause scenario, according to which flares and CMEs are different manifestations of the same large-scale magnetic process on the star (Zhang et al., 2001). Though the details of this process still remain unclear, already now it can be definitely stated that an intensive flaring activity of a star should be accompanied by an increased rate of CME production. The probability of CME–flare association increases with a duration of a flare (Sheeley et al., 1983): ~26% for flare duration <1 h; and 100% for flare duration >6 h.

Multi-thermal structure of CMEs includes (1) coronal material in the front region (~2 MK); (2) a core formed by prominence material (~8000 K), or hot flare plasma (~10 MK). The temperatures given here correspond to the typical temperatures in the case of the Sun. They can be different for other stars. CME/ICME structure evolves during its propagation in the interplanetary space. The following sequence of structures can be related to the ICMEs: (1) interplanetary shock, (2) sheath, and (3) the ICME itself. The ejecta can contain ordered magnetic field, in which case it is termed as a magnetic cloud (MC) (Burlaga et al., 1981). MCs constitute a subset of all ejecta (about 33%).

2.2. CME velocity and acceleration

The basic and widely considered characteristic of CMEs is their velocity v_{CME}, determined by the tracking of a CME feature in coronagraph image frames taken with a certain time cadence. According to the data from SoHO/LASCO the velocity of solar CMEs ranges from tens of km s^{-1} to >2500 km s^{-1}, with an average value of about 490 km s^{-1} (e.g., Gopalswamy, 2004). Due to the relatively large statistics (>8000) of the considered SoHO/LASCO CMEs, the average ejecta velocity value can be considered as a representative quantity. It is also consistent with the results of other velocity measurement techniques applied to separate CME phenomena (Lindsay et al., 1999; Gopalswamy et al., 2000, 2001a, b; Lara et al., 2004).

Observations of solar CMEs reveal also that they appear to be subject to various forces, and experience certain acceleration a, which changes during their travel in the interplanetary space. In general, the dynamics of CMEs can be governed by the three main forces: (i) a not well understood propelling force, (ii) the gravity force, and (iii) a kind of restraining force, which is caused probably by interaction with the background medium. Based on the observational data from SoHO, Gopalswamy et al. (2000) derived an empirical linear dependence of the interplanetary acceleration of a CME on its speed near the Sun: $a = a(v_{\mathrm{CME}})$ (see also Gopalswamy et al., 2002). This can be used to get the velocity of an ICME at a given orbital distance d : $v_{\mathrm{ICME}} = (v_{\mathrm{CME}}^2 + 2ad)^{1/2}$. However, at close distances near the star, change of a CME speed is not very significant. This makes it not important for the study of

effects produced by CMEs on the magnetospheres and atmospheres of close-orbit exoplanets like HD209458b. Thus, in the present paper we use everywhere a constant value close to the average velocity of solar CMEs.

2.3. CME size and latitude distribution

The CME angular width Δ_{CME} is measured as the position angle extent of the ejecta in the sky plane. It can be also a subject to projection effect errors. Δ_{CME} increases on the initial stages of propagation ($<5R_{Sun}$) and then remains usually constant. Annual average Δ_{CME} of non-halo CMEs ranges from 45° (solar minimum) to 61° (close before activity maximum) (Gopalswamy, 2004; Yashiro et al., 2004).

The latitude distribution of CMEs depends on the distribution of closed field magnetic regions related to active areas on the solar surface (Hundhausen, 1993; Gopalswamy et al., 2003a). During the rising phase of solar activity cycle, CME latitudes spread gradually from those close to the equator (0°) up to all latitudes (±90°). At the same time, the majority of eruptions were located within the average latitude interval $\pm\Theta$ near the equatorial plane, with $\Theta = 60°$ (Gopalswamy, 2003, 2004).

2.4. CME occurrence rate

An important characteristic of the CME activity of the Sun is the ejection frequency f_{CME} of CMEs, or the CME occurrence rate. The data from Skylab, SMM, Helios, Solwind, and SoHO indicate certain correlation between sunspot numbers (SSN) and the CME occurrence rate (Hildner et al., 1976; Howard et al., 1986; Webb and Howard, 1994; Cliver et al., 1994; St. Cyr et al., 2000; Gopalswamy et al., 2003b). At the same time, SoHO/LASCO observations found that although there is an overall similarity between the SSN and the CME occurrence rates, there are some differences in details.

The most recent SoHO/LASCO observations give a CME occurrence rate $f_{CME} \approx 0.8$ CMEs/day ≈ 0.033 CMEs/hour for solar minimum and $f_{CME} \geqslant 6$ CMEs/day $=$ 0.25 CMEs/hour for solar maximum (St. Cyr et al., 2000; Gopalswamy, 2004). These numbers are consistent, but a bit higher as compared to previous estimations (Hildner et al., 1976; Webb and Howard, 1994, Cliver et al., 1994), which is attributed to the better sensitivity and the high dynamic range of the LASCO coronagraphs.

2.5. CME and ICME plasma density as a function of orbital distance

For studying the effects produced by collisions of CMEs and ICMEs with planetary environments, it is important to know how the CME and ICME plasma density n_{CME} changes as a function of orbital distance d. CME density at distances $\leqslant 30R_{Sun} \approx 0.14$ AU is estimated from the analysis of associated CME brightness enhancements in the white-light coronagraph images.

Estimates of CME plasma density n_{CME} from white light (Vourlidas et al., 2002), radio (Gopalswamy and Kundu, 1993), and UV observations (Ciaravella et al., 2003) give at distances $\approx 3-5r_{Sun}$ similar values of about $10^6\,cm^{-3}$, which are consistent with the assumption of the coronal value of density of a CME material at the moment of ejection. Based on the white-light coronagraphs images from SoHO/LASCO, Lara et al. (2004) derived the following empirical power-law dependence for the density of CME material at the orbital distance d from the Sun:

$$n_{CME} = n^0_{CME}\left(\frac{d}{d_0}\right)^{\kappa}, \quad (1)$$

where n^0_{CME} is the density of a CME near the Sun at distance d_0, and $\kappa = -3.6$ is empirically determined power-law index. With n^0_{CME} in a range between 5×10^5 and $5\times10^6\,cm^{-3}$ and $d_0 \approx (3-5)r_{Sun} = (0.014-0.023)$ AU, this power-law dependence gives a good approximation for the CME density variation within the distances range $\leqslant 20r_{Sun} \approx 0.1$ AU. In addition, Lara et al. (2004) report about the average duration of CMEs in the $6r_{Sun}-10r_{Sun}$ interval to be $t_{CME} \approx 8$ h. This time is consistent with the measured characteristic spatial scales and velocities of ejecta.

At larger distances in the outer heliosphere $>30r_{Sun}$, i.e. >0.14 AU, the density and duration of ICMEs and associated MCs are measured in situ by spacecraft (Henke et al., 1998; Lepri et al., 2001). For the plasma density in MCs observed between 0.3 and 1 AU by the Helios satellites, Bothmer and Schwenn (1998) found a power law

$$n_{MC} = n^0_{MC}\left(\frac{d}{d_0}\right)^{(-2.4\pm0.3)}, \quad (2)$$

where d is the radial distance to the Sun in units of AU, quantity $n^0_{MC} = 6.47 \pm 0.95\,cm^{-3}$ is the MC plasma density at the near-Earth distance, and $d_0 = 1$ AU (Bothmer and Schwenn, 1998).

3. Extrapolation of the solar CME parameters to an extrasolar case

An application of the average solar CME/ICME parameters and estimations, such as velocities v_{CME}, v_{ICME}, plasma densities n_{CME}, n_{MC}, size Δ_{CME}, occurrence rate f_{CME}, duration time t_{CME}, and the latitude interval 2Θ, to other stars should be performed with a certain care. Because stellar winds are poorly known we cannot obtain the precise properties of CMEs and ICMEs at particular orbital distances at an other star. Our approach consists in using the Sun as a typical example of a G-type star with an age of about 4.0–5.0 Gyr. This solar–stellar similarity assumption allows us to study collisions between "Hot Jupiters" and stellar CMEs, applying known relationships between the flaring and CME activities at the Sun, as well as the solar CME parameters, taken within a reasonable minimum-maximum range.

Since the fundamental physical mechanisms, responsible for the initiation and ejection of CMEs, should not be different for similar G-type stars, it is very likely that plasma densities and velocities of extra-solar and solar CMEs will be close to each other. Therefore, as a reasonable approximation in our calculations we take for the velocity of the extra-solar ejecta, which impacts a short periodic exoplanet like HD2094598b at 0.045 AU orbiting an about 4.0–5.0 Gyr old G-type star, the value $v_{CME} = 500\,km\,s^{-1}$.

Based on Eqs. (1) and (2) we produce a general fit of the CME and ICME plasma density variation over the orbital distances from 0.014 to 1 AU:

$$n_{CME}^{min} = n_0^{min}\left(\frac{d}{d_0}\right)^{-2.3}, \quad (3)$$

$$n_{CME}^{max} = n_0^{max}\left(\frac{d}{d_0}\right)^{-3.0}, \quad (4)$$

where $n_0^{min} = 4.88\,cm^{-3}$, quantity $n_0^{max} = 7.1\,cm^{-3}$, $d_0 = 1\,AU$, and d is the radial distance from the star measured in AU. In this fit we cover analogous to the Sun reasonable interval of CME/ICME plasma densities, which at the orbital distances <0.1 AU is defined by Eq. (1), with $n_{CME}^0 = 5\times10^5 - 5\times10^6\,cm^{-3}$ and $d_0 = 3r_{Sun} = 0.014$, whereas at distances between 0.3 and 1 AU we take into account a certain dispersion of the in situ measured ICME plasma densities described by Eq. (2).

Fig. 1 shows the derived minimum and maximum CME number density as a function of orbital distance from the host star. One can see that the number density of the CME plasma at orbital distances HD20945b of about 0.045 AU can reach very high values of about 6.3×10^3–$7.5\times10^4\,cm^{-3}$, which should cause a strong impact on the short-periodic exoplanet magnetosphere and atmosphere if it collides with a CME.

As additional important factors for planetary collisions with CMEs appear the interaction time period of CME plasma with the exoplanet and the frequency at which CMEs may hit a "Hot Jupiter" at close orbital distances. Fig. 2 illustrates the geometrical scheme which can be used for the estimation of the probability of collision between CMEs and "Hot Jupiters". In our calculations of the planetary magnetospheric and atmospheric effects produced by CMEs we assume that the duration of each CME, as it passes over the exoplanet, is long enough in comparison with the characteristic transition and magnetospheric reconfiguration process time scales. In such a case the CME—exoplanet interaction can be modelled as an interaction of the exoplanet with a stellar wind, which has density and velocity specific for the CME. Such an approach seems to be reasonable in view of the fact that the average interaction time period of CMEs t_{CME} is several hours, whereas the typical time t of the magnetosphere/atmosphere reaction to disturbed parameters like density and velocity of the stellar wind is about several minutes (Arshukova et al., 2004; Penz et al., 2004). After a CME has passed the close-in exoplanet, the parameters of the stellar wind are restored to the regular ones.

Assuming a strictly radial propagation of CMEs from a star, and taking into account the fact that CMEs have a certain angular size Δ_{CME} and are distributed within a certain latitude interval $\pm\Theta$ near the equatorial plane of the host star, the impact frequency f_{imp} at which CMEs hit an exoplanet of an angular size δ_{pl} can be calculated by the following expression:

$$f_{imp} = \frac{(\Delta_{CME} + \delta_{pl})\sin[(\Delta_{CME} + \delta_{pl})/2]}{2\pi\sin\Theta} f_{CME}, \quad (5)$$

where f_{CME} is the CME production rate (ejection frequency) by the star and the coefficient in front of it defines the probability that an ejected CME collides with the "Hot Jupiter". This coefficient is obtained as a product of probabilities of a CME to be ejected within the correct meridional, $\pi/2-(\Delta_{CME}+\delta_{pl})/2<\Theta<\pi/2+(\Delta_{CME}+\delta_{pl})/2$, and azimuthal, $-(\Delta_{CME}+\delta_{pl})/2<\varphi<(\Delta_{CME}+\delta_{pl})/2$, angles, which allow at least a short interaction between a CME and a planet. By this, the planet is assumed to orbit the star in the ecliptic plane ($\Theta = \pi/2$) as shown in Fig. 2.

Assuming an average CME occurrence rate of about 3 CMEs per day (cf. Section 2.4) and taking the size, duration and latitude distribution of CMEs to be close to the solar values ($\Delta_{CME} = \pi/4 - \pi/3$, $t_{CME} = 8\,h$, $\Theta = \pi/3$), which should also be a reasonable approximation for the 4.0–5.0 Gyr old solar-like G-type host star of HD209458b with the angular size $\delta_{pl} = 0.0212$ rad, one obtains a CME impact rate of about 0.17–0.3 hits per day.

Table 1 summarizes the average CME velocity, size Δ_{CME}, occurrence rate f_{CME}, CME exposure time t_{CME}, impact rate f_{imp}, minimum and maximum CME plasma density n_{CME}^{min} and n_{CME}^{max} at the orbital distance of HD209458b of about 0.045 AU. Since the orbital period of HD209458b around its host star is about 3.5 days, it follows that this exoplanet should collide with a CME, approximately once at each orbital period.

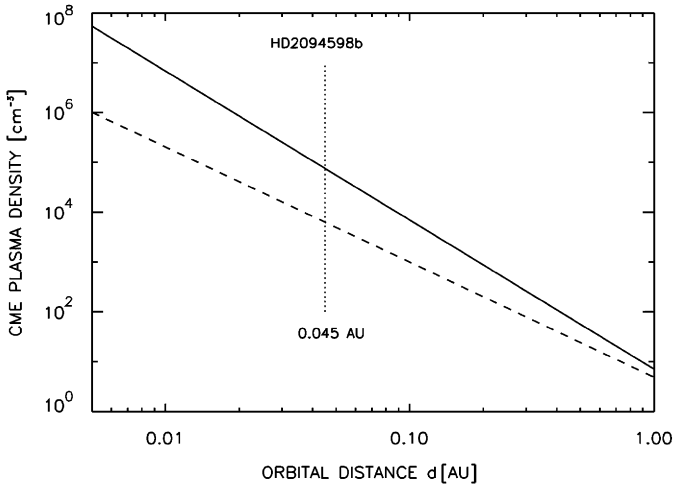

Fig. 1. Minimum (dashed-line) and maximum (solid-line) CME and ICME plasma density as a function of orbital distance.

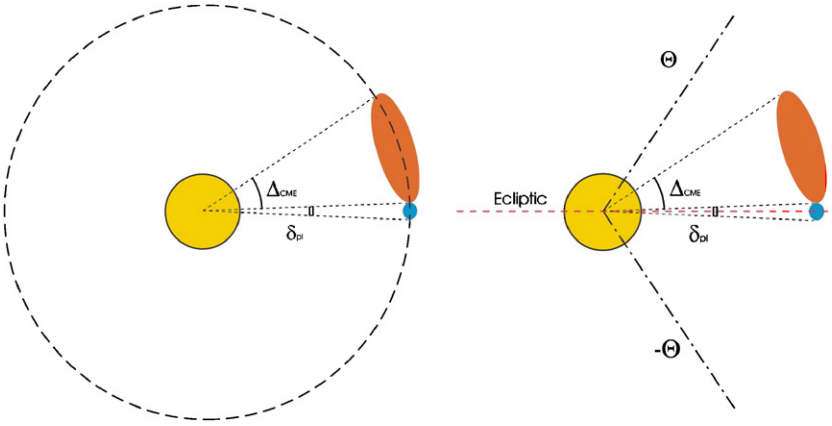

Fig. 2. Schematic illustration of collisions between a CME and "Hot Jupiters". Azimuthal plane view (left) and meridional plane view (right). Δ_{CME} is the angular size of the CME, δ_{pl} is the angular size of the exoplanet, and Θ is the angle within which CMEs are ejected from the star.

Table 1
Expected CME parameters at HD209458b's orbital distance of about 0.045 AU

v_{CME} (km s^{-1})	Δ_{CME}	f_{CME} (day^{-1})	t_{CME} (h)	f_{imp} (day^{-1})	n^{min}_{CME} (cm^{-3})	n^{max}_{CME} (cm^{-3})
490	45°–60°	3	8	0.17–0.3	≈ 6300	≈ 7.5×10^4

4. CME plasma interaction with the evaporating hydrogen atmosphere of HD209458b

Applying the scaling laws based on analytical models which allow an estimation of a planetary magnetic dipole moment parallel to the rotation axis, Grießmeier et al. (2004) calculated the interval of plausible values for the magnetic moment of HD209458b. For slow rotating "Hot Jupiters" like HD209458b this interval of expected magnetic moments appeared as 0.005–0.1$\mathscr{M}_{Jup}$. Similarly, the estimations of Sánchez-Lavega (2004) indicate that "Hot Jupiters" have a strongly reduced magnetic field due to their slow rotation. Since the exact topology of magnetospheres of exoplanets is unknown, one can use only simplified models to get a rough estimation about the magnetospheric shape of such planets. Grießmeier et al. (2004) used for the modelling of magnetospheric magnetic fields of "Hot Jupiters" the parametric model developed by Voigt (1981) and generalized by Stadelmann (2004). The shape of such magnetospheres is not self-consistent. It is approximated by a semi-infinite cylinder on the nightside and by a half-sphere on the dayside. Both magnetospheric structures have approximately the same radius r_m. The planet is placed within the half-sphere at a stand-off distance $r_s = 0.5r_m$. The stand-off distance r_s between the stellar wind or, in our case, the CME plasma flow and the planetary magnetic moment is determined from the ram pressure balance condition at the substellar point, which yields the following expression (Grießmeier et al., 2004):

$$r_s = \left[\frac{\mu_0^2 f_0^2 \mathscr{M}^2}{8\pi^2 \mu_0 n_{CME} m v_{CME}^2}\right]^{1/6}, \quad (6)$$

where $\mathscr{M}$ is the planetary magnetic moment, m is proton mass, μ_0 and f_0 are the magnetic permeability and a magnetospheric form factor, respectively.

As was mentioned above, there is an evidence from HST observations (Vidal-Madjar et al., 2003, 2004) and theoretical considerations (Lammer et al., 2003a; Yelle, 2004; Tian et al., 2005; Langmayr et al., 2006) that upper atmospheres of "Hot Jupiters" experience hydrodynamic blow-off. To study the interaction between the hydrodynamically driven planetary neutral hydrogen wind in HD209458b and the CME plasma flow, we apply the hydrodynamic numerical model described in detail in Langmayr et al. (2006). Numeric solution of the system of hydrodynamic equations is obtained within two steps: (1) the continuity and momentum equations are solved together by Godunov's method, and (2) the temperature is included via a leap frog step. The main advantage of this procedure is that it allows an accurate treatment of the occurring strong gradients, in particular close to the exoplanet.

Vidal-Madjar et al. (2003, 2004) inferred from their Lyman-α absorption observations on HD209458b with the space telescope imaging spectrograph (STIS) on board of the hubble space telescope (HST) at about $2.5r_{pl}$ a reference H number density of about $\geqslant 10^6$ cm^{-3}. However, Vidal-Madjar et al. (2003, 2004) noted that due to saturation effects in the Lyman-α absorption line of their observations, densities which are several orders of magnitude higher would produce similar absorption signatures. To be consistent with this observation and previous model calculations by Yelle (2004) and Tian et al. (2005) we use in our calculation of the neutral density profile a density value of 10^6 cm^{-3} as an initial condition at $2.5r_{pl}$.

The difference between the density profile calculated in this work and shown in Fig. 3 and that one obtained by Erkaev et al. (2005) is caused by the fact that the profile of the hydrogen particle population was calculated by Erkaev et al. (2005) using the Monte Carlo Model of Wurz and Lammer (2003) and assuming a Maxwell-type velocity distribution as well as a main temperature of about 10 000 K at a planetocentric distance of about $3r_{pl}$ (Vidal-Madjar et al., 2003; Lecavlier des Etangs et al., 2004). The hydrogen number density at this altitude was estimated to be about $10^5\,cm^{-3}$.

The dotted and dashed lines in Fig. 3 represent the magnetopause stand-off distance corresponding to the minimum and maximum CME plasma density and the maximal estimated planetary magnetic moment of HD209458b $\mathcal{M}_{max} = 0.1\mathcal{M}_{Jup}$. Similar calculations but with the minimal estimated planetary magnetic moment $\mathcal{M}_{min} = 0.005\mathcal{M}_{Jup}$ give magnetic stand-off distances of about 0.56–0.8r_{pl}. These stand-off distances lie below the visual radius ($r/r_{pl} = 1.0$) of HD209458b. Since at the deep atmospheric levels the neutral gas density is very high, we expect that the CME plasma flow will be deflected around the planet at somewhat higher distances which is shown as a shaded area in Fig. 3. In such cases we assume that dense CME plasma flow may interact with the atmospheric neutral gas between 1.0 and $1.3r_{pl}$ where it ionizes the neutrals mainly due to collisions so that a Venus-like ionopause transition region will form. To study relation between possible CME penetration depths and the efficiency of planetary atmospheric erosion we calculate the minimum and maximum ion mass loss rates for different sizes of the planetary obstacles: 2.33, 1.54, 1.3, 1.15 and $1.0r_{pl}$.

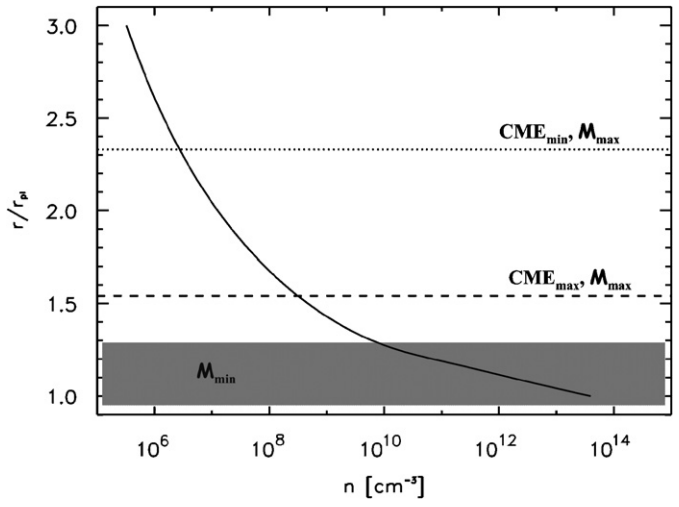

Fig. 3. Neutral hydrogen density profile of the upper atmosphere under hydrodynamic conditions of HD209458b as a function of planetocentric distance in units of planetary radii. The dotted and dashed lines mark the magnetopause stand-off distance corresponding to the minimum and maximum CME plasma densities, respectively, and the maximum expected magnetic moment $\mathcal{M}_{max} = 0.1\mathcal{M}_{Jup}$. In the case of the minimum expected magnetic moment of HD209458b $\mathcal{M}_{min} = 0.005\mathcal{M}_{Jup}$, the magnetopause stand-off distances would lay below the visual planetary radius at about 0.56–0.8r_{pl}. Since at deep atmospheric levels the neutral gas density is very high, one can expect that the CME plasma flow will be deflected around the planet at somewhat higher altitudes which are shown as a shaded area.

We considered the hydrogen ion pick-up loss rates caused by the CME plasma flow, taking into account the ionization processes produced by CMEs during the interaction with the neutral atmosphere. The numerical test particle model applied in this study (Lichtenegger and Dubinin, 1998; Lichtenegger et al., 2002) was successfully used for the simulation of ion pick-up loss rates from various planetary atmospheres (Luhmann, 1993; Lichtenegger et al., 1995; Lichtenegger and Dubinin, 1998; Lammer et al., 2003b; Erkaev et al., 2005).

The total production rate of planetary H^+ ions is the sum of the rates of photo-ionization, electron impact ionization, and charge exchange. In the reaction between CME protons and the evaporating planetary hydrogen atoms, the energy dependent charge exchange cross section was applied (Kallio and Luhmann, 1997). Simulation of the particle fluxes is initialized by dividing the space around the planetary obstacle onto a number of volume elements ΔV. Production rates of planetary H^+ ions are obtained by calculation of the absorption of the CME plasma flow along streamlines due to the charge exchange with the evaporating atmospheric neutral gas. The CME plasma flux Φ_{CME} in a volume element ΔV_i at a given position $\boldsymbol{r}_i$ with respect to the planetary center is determined by

$$\Phi_{CME}(\boldsymbol{r}_i) = \Phi^{(0)}_{CME}(\boldsymbol{r}_i) e^{-\int_{\infty}^{s_i} \sum_H n_H \sigma_H \, ds}, \quad (7)$$

where the integration is performed from the upstream CME plasma flow to the corresponding point s_i at position $\boldsymbol{r}_i$ on the streamline. $\Phi^{(0)}_{CME}$ is the unperturbed CME plasma flux, n_H is the neutral hydrogen density as a function of planetary distance, σ_H is the energy dependent charge exchange cross section between a proton and the neutral hydrogen atom, and ds is the line element along the streamline. The loss rate of CME protons in units of $cm^{-3}\,s^{-1}$ due to the interaction with the evaporating atmosphere is $l^H_{CME} = \Phi_{CME} n_H \sigma_H$. The corresponding planetary H^+ ion production rate $p^{ce}_{H^+}$ due to charge exchange is assumed to be equal to the corresponding loss rate of the CME protons, i.e., $p^{ce}_{H^+} = l^H_{CME}$. The rate of H^+ ions produced by electron impact is given by $p^{ei}_{H^+} = \nu n_e n_H$, where ν is a temperature dependent ionization frequency per incident electron and n_e is the electron density. The total planetary ion production rate from the atmospheric hydrogen atoms in each volume element is the sum $p^{tot}_{H^+} = p^{ei}_{H^+} + p^{ce}_{H^+} + p^{\gamma}_{H^+}$, with $p^{\gamma}_{H^+}$ being the rate due to photo-ionization.

Table 2 shows for HD209458b the calculated H^+ ion pick-up loss rates S in units of s^{-1} and mass loss rates L in units of $g\,s^{-1}$ for the minimum and maximum CME plasma densities and expected magnetopause stand-off distances r_s given in planetary radii. One can see that our calculations yield H^+ ion pick-up loss rates of about $1.5 \times 10^{11}\,g\,s^{-1}$

Table 2
H^+ ion loss rates on HD209458b due to its interaction with CMEs, for different CME plasma densities and expected planetary magnetic moments

Conditions	S (s^{-1})	L ($g\,s^{-1}$)	$\mathcal{M}$ ($\mathcal{M}_{Jup}$)	n_{CME} (cm^{-3})	r_s (r_{pl})	$\Gamma(M_{pl})$
CME_{min}, $\mathcal{M}_{max}$	9×10^{34}	1.5×10^{11}	0.1	6300.0	2.33	1.56×10^{-2}
CME_{max}, $\mathcal{M}_{max}$	7×10^{37}	2×10^{13}	0.1	7.5×10^4	1.54	0.2
CME_{min}	7.2×10^{36}	1.2×10^{13}	0.017	6300.0	1.3	0.12
CME_{max}	8.2×10^{37}	1.37×10^{14}	0.059	7.5×10^4	1.3	1.43
CME_{min}	8.4×10^{37}	1.4×10^{14}	0.012	6300.0	1.15	1.46
CME_{max}	9.5×10^{38}	1.6×10^{15}	0.041	7.5×10^4	1.15	17.0
CME_{min},$\mathcal{M}_{min}$	5.0×10^{39}	8.35×10^{15}	0.005	6300.0	1.0 [0.85]	87.0
CME_{max}, $\mathcal{M}_{min}$	5.7×10^{40}	9.5×10^{16}	0.005	7.5×10^4	1.0 [0.56]	990.0

during a CME exposure period, even in the case of the minimum CME plasma density and the maximum expected magnetic moment. In the case of the maximum CME plasma density and the maximum expected magnetic moment the loss rates are in the order of about $2.0 \times 10^{13}\,g\,s^{-1}$. This higher loss rate is related with the stronger compression of the magnetosphere, which results in a closer magnetopause stand-off distance. The obtained H^+ ion mass loss rates during a CME plasma interaction with HD209458b can be several orders of magnitude larger than during usual stellar wind interaction studied by Erkaev et al. (2005) and estimated by Guillot et al. (1996).

Furthermore, one can see from Table 2 that the H^+ ion pick-up loss rates get larger if the planetary obstacle of the CME plasma flow is assumed at closer distances to HD209458b's visual radius r_{pl}. Since HD209458b orbits every 3.5 days around a G-type star similar to the Sun, one can estimate from the parameters in Table 1 that the exoplanet collides with a CME at least once per each rotation period. This results in about 5×10^{11} CME hits over the exoplanet's lifetime, even if we take a very conservative assumption that the average CME occurrence rate was always similar and never higher than that of the present Sun. Finally, taking the average duration of CMEs $t_{CME} \approx 8\,h$ as the typical exposure time during which the atmospheric erosion acts during a collision, one will obtain a total duration of CME plasma–magnetosphere–atmosphere interaction $t_{ip} \approx 1.44 \times 10^{16}\,s$. Using this value and assuming that HD209458b is protected by the maximal expected magnetic moment of about $0.1\mathcal{M}_{Jup}$ with magnetospheric stand-off distances $r_s = 1.54$–2.33 one obtains total mass loss rates $\Gamma = 1.2 \times 10^{-2} - 0.2\,M_{pl}$ over the exoplanet's history. Applying t_{ip} together with the ion loss rates L ($g\,s^{-1}$) corresponding to different CME densities and planetary magnetic moments as shown in Table 2, we find that the atmospheric erosion caused by CMEs becomes important for evolutionary mass loss aspects if the atmospheric loss rate is $\geqslant 10^{13}\,g\,s^{-1}$. In particular, for mass loss rates L ($g\,s^{-1}$) of about 1.2×10^{13}, 2.0×10^{13}, 1.4×10^{14}, 1.6×10^{15}, 8.35×10^{15}, and $9.5 \times 10^{16}\,g\,s^{-1}$, HD209458b would have lost about 0.12, 0.2, 1.46, 17, 87, and $990 M_{pl}$ over its lifetime (see Table 2). Since it is rather unrealistic that HD209458b has lost much more than its present mass, the planetary obstacle which deflects the CME plasma flow should occur at least at 1.3–$1.5 r_{pl}$ or even at larger distances above its visual radius.

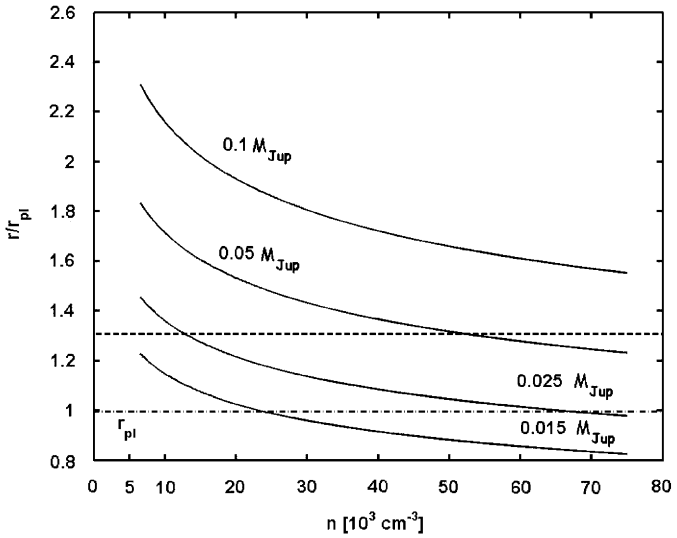

Fig. 4. Magnetopause stand-off distance in planetary radii as a function of minimum and maximum CME plasma density at HD209458b's orbital distance of about 0.045 AU and various possible magnetic moments. Planetary obstacles below the dashed line result in "non-negligible" atmospheric mass loss rates over the evolutionary time periods. The dashed-dotted line corresponds to the visual planetary radius of HD209458b, which is about $1.43 r_{Jup}$.

Fig. 4 shows the expected magnetospheric stand-off distance for HD209458b in units of planetary radii as a function of the minimum and maximum CME density at orbital distances of about 0.045 AU and magnetic moments of 0.1, 0.05, 0.025, and $0.015\mathcal{M}_{Jup}$. Stand-off distances below the dashed line will have strong impacts on the atmospheric evolution and mass loss of HD209458b and similar "Hot Jupiters". Thus, the fact that such planets are still observable may be related to intrinsic magnetic moments which are strong enough to protect the planetary atmospheres against collisions with CMEs. On the other hand, decreased mass loss rates may take place not only due to an efficient magnetospheric, but also due to a lower CME activity of the planets' host stars. This fact may provide a certain constrain to the CME activity rates of the

solar-type stars which nowadays is based only on the direct analogy with the Sun and its known flaring and CME activity.

5. Implications for atmospheric evolution and "Hot Jupiters" discovered by CoRoT

Because the radiation and particle flux of a host star plays a major role in all atmospheric loss processes, the evolution of planetary atmospheres must be considered within the context of the evolving stellar energy and particle fluxes. Observations of radiative fluxes, stellar magnetic fields, and stellar winds on solar-type stars with different ages (Zahnle and Walker, 1982; Ayres, 1997; Guinan and Ribas, 2002; Wood et al., 2002, 2005; Ribas et al., 2005) indicate that our young Sun underwent a highly active phase after its formation. This active phase of the Sun, which lasted about 0.5–1.0 Gyr after its arrival on the Zero-Age-Main-Sequence (ZAMS), included continuous flare events where the particle and radiation environment was several hundred times more intense than today. The high radiation levels of the young Sun were triggered by strong magnetic activity. The magnetic activity of the Sun is expected to have greatly decreased with time (Skumanich, 1972; Simon et al., 1985; Guinan and Ribas, 2002) as the solar rotation slowed down through angular momentum loss. Observational evidence and theoretical models suggest that the young Sun rotated about 10 times faster than today and had significantly enhanced magnetically generated coronal, chromospheric, and CME activity (Keppens et al., 1995; Guinan and Ribas, 2002; Ribas et al., 2005).

From the observations of young solar-like stars one can conclude that the G-type host star of HD209458b also experienced a highly active period with probably higher CME occurrence rates than observed at the present Sun. This enhanced activity would also enhance the mass loss of the exoplanet unless its upper atmosphere is protected by a strong intrinsic magnetic moment which builds up a magnetospheric stand-off distance $r_s \geqslant 1.3$–$1.5 r_{pl}$. Our results indicate that the calculated CME-caused atmospheric loss rate depends strongly on the altitude of the planetary obstacle since more neutral gas can be picked up by the CME plasma flow around HD209458b when the obstacle boundary is deeper in the atmosphere.

At the present stage of our model investigations for weakly magnetized "Hot Jupiters" we cannot calculate or estimate an accurate atmospheric altitude where dense and fast CME plasma fluxes can be deflected around a Venus-like ionopause. If future studies, focused on the modelling of the formation of CME-induced ionized/magnetized planetary obstacles around weakly magnetized "short-periodic" gas giants, will find that the CME plasma flow is deflected around planetocentric distances $\leqslant 1.3 r_{pl}$, exoplanets with such CME plasma-interaction should experience a huge mass loss over their history and can even be eroded down to their core size. On the other hand, such results would indicate that "Hot Jupiters", which are currently detected at very short orbital distances like HD209458b, OGLE-TR-56b, OGLE-TR-113b, OGLE-TR-132b, etc. by assuming a solar type CME activity of their host stars, might have strong enough magnetic moments, which balance the CME plasma pressure at planetocentric distances $\geqslant 1.3$–$1.5 r_{pl}$ and prevent catastrophic atmospheric erosion.

More detailed investigations of the dense CME plasma interaction with weakly magnetized "Hot Jupiters" have to be carried out in the future, because large atmospheric mass loss of "Hot Jupiters" leads to the existence of a critical mass for a given orbital distance below which the evaporation time scale becomes shorter than the thermal time scale (Baraffe et al., 2004). In cases of exoplanets with initial masses below this critical one, atmospheric loss can lead to a rapid expansion of the outer layers and of the total planetary radius, speeding up the mass loss process. In such a stage, the "Hot Jupiter" does not survive as long as estimated by a simple application of mass loss rates without following consistently its evolution. Baraffe et al. (2004) note that HD209458b because of its radius–mass discrepancy might be in such a dramatic phase, although with an extremely small probability.

More phenomenological information, important for the study of the efficiency of the atmospheric mass loss of "Hot Jupiters", as well as about their host star activity, is expected from the CoRoT space observatory, which may discover about 200 hot exoplanets with masses $\geqslant 0.1 M_{Jup}$ and orbital periods <10 days (Moutou et al., 2003).

If the interaction of CME plasma with the magnetospheric and atmospheric environments of "Hot Jupiters" is efficient enough our study suggests that CoRoT together with ground-based follow-up observations will discover several smaller-size/mass objects very close to their host stars. These objects could be the remnants of evaporated and eroded "Hot Jupiters". It is also possible that CME-induced non-thermal mass loss processes together with hydrodynamic evaporation (e.g., Lammer et al., 2003a; Baraffe et al., 2004; Langmayr et al., 2006), and tidal interactions (Pätzold and Rauer, 2002) are a reason that so far no "Hot Jupiter" is observed at orbital distances $\leqslant 0.0225$ AU.

6. Conclusions

We investigated for the first time atmospheric erosion due to CME-caused ion pick-up on "Hot Jupiters", by using as an example the $0.69 M_{Jup}$ gas giant HD209458b. Our results indicate that this exoplanet and similar short-periodic slow rotating "Hot Jupiters" at orbital distances $\leqslant 0.05$ AU around solar-like stars with ages comparable to our Sun may experience strong atmospheric mass loss related to CME plasma interaction with their magnetospheric–atmospheric environments. The mass loss depends on the magnetic moment of these exoplanets, which was expected to be at least in the range of about 0.005–$0.1 \mathcal{M}_{Jup}$

(Grießmeier et al., 2004). If HD209458b is protected by a magnetic moment of about $0.1\mathscr{M}_{Jup}$ the CME plasma flow would be deflected around the exoplanet at planetocentric distances of about $1.54–2.33r_{pl}$. We found that the CME plasma flow will erode the hydrodynamically evaporating neutral upper atmosphere of HD209458b at a rate of about $1.5\times10^{11}–2.0\times10^{13}\,g\,s^{-1}$. Weaker magnetic moments are able to balance the CME plasma flow only at planetocentric distances $\leqslant1.54r_{pl}$ which results in larger mass loss rates. We expect that the atmospheres of weakly magnetized "Hot Jupiters" will be ionized by the penetrating CME plasma flow which will form a Venus-like planetary obstacle closer to the visual radius of the exoplanet. Calculations of the CME-caused atmospheric H^+ ion pick-up loss rate of HD209458b over its lifetime, by assuming the observed solar CME occurrence rate, show that if the CME plasma flux is deflected at distances $<1.3r_{pl}$, then the planet can be eroded down to their core sizes. Since HD209458b at 0.045 AU or OGLE-TR-56b at about 0.0225 AU have masses of 0.69 and $1.45M_{Jup}$, respectively, we expect that these exoplanets, as well as other "Hot Jupiters" observed at such close orbital distances, might have strong enough magnetic moments which are able to keep the magnetospheric stand-off distances at high enough altitudes where the interaction of the CME plasma with planetary atmosphere is not so efficient. Future studies related to the interaction between the CME plasma flux and "Hot Jupiters" should focus on the formation of planetary obstacles around weakly magnetized exoplanets. These studies are important for a better understanding of the mass loss processes on "Hot Jupiters" and close-in exoplanets in general.

Acknowledgments

The data about the main statistical features of the solar CMEs used in this paper are based on the CME catalog, generated and maintained by NASA and The Catholic University of America in cooperation with the Naval Research Laboratory (http://cdaw.gsfc.nasa.gov/CME_list/). M.L. Khodachenko acknowledges support from the Austrian "Fonds zur Förderung der wissenschaftlichen Forschung" (FWF) (project P16919-N08), ÖAD-RFBR Scientific and Technical Collaboration Program (project No. I. 21/04), and the ÖAD-Acciones Integradas Program (project No. 11/2005). H. Lammer acknowledges also support by the ÖAD-Acciones Integradas Program (project No. 12/2005). M. Leitner, T. Penz, H.K. Biernat, H. Lammer, D. Langmayr, and N.V. Erkaev acknowledge support by the FWF under projects P17099-N08 and P17100-N08, by the INTAS–ESA Project 99-01277, and by the RFBR-grant 03-05-20014_BNTS_a as well as by grants 04-05-64088, 05-02-16252. The authors thank also the Austrian Academy of Sciences "Verwaltungsstelle für Auslandsbeziehungen" the Austrian Ministry for Science, Education and Culture (bm:bwk) and ASA for funding the CoRoT project. This study was supported by the International Space Science Institute (ISSI) and carried out in the framework of the ISSI Team "Formation, Structure and Evolution of Giant Planets". We would like also to give our special thanks to P. Odert and M. Leitzinger for their helpful consultations and assistance.

References

Arshukova, I.L., Erkaev, N.V., Biernat, H.K., Vogl, D.F., 2004. Interchange instability of the Venusian ionopause. Adv. Space Res. 33, 182–186.

Ayres, T.R., 1997. Evolution of the solar ionizing flux. J. Geophys. Res. 102, 1641–1651.

Baraffe, I., Selsis, F., Chabrier, G., Barman, T.S., Allard, F., Hauschildt, P.H., Lammer, H., 2004. The effect of thermal escape on the evolution of close-in giant planets. Astron. Astrophys. 419, L13–L16.

Barman, T.S., Hauschildt, P.H., Schweitzer, A.S., Phillip, C., Baron, E., Allard, F., 2002. Non-LTE effects of Na I in the atmosphere of HD209458b. Astrophys. J. 569, L51–L54.

Bothmer, V., Schwenn, R., 1998. The structure and origin of magnetic clouds in the solar wind. Ann. Geophys. 16, 1–24.

Burlaga, L.F., Sittler, E., Mariani, F., Schwenn, R., 1981. Magnetic loop behind an interplanetary shock—Voyager, Helios, and IMP 8 observations. J. Geophys. Res. 86, 6673–6684.

Ciaravella, A., Raymond, J.C., van Ballegooijen, A., Strachan, L., Vourlidas, A., Li, J., Chen, J., Panasyuk, A., 2003. Physical parameters of the 2000 February 11 coronal mass ejection: ultraviolet spectra versus white-light images. Astrophys. J. 597, 1118–1134.

Cliver, E.W., St. Cyr, O.C., Howard, R.A., Mc Intosh, P.S., 1994. Rotation-averaged rates of coronal mass ejections and dynamics of polar crown filaments. In: Rusin, V., Heinzel, P., Vial, J.-C. (Eds.), Solar Coronal Structures. Proceedings of the 144th IAU Colloquium, Tatranska Lomnica, Slovakia, September 20–14, 1993. VEDA Publishing House of the Slovak Academy of Sciences, pp. 83–89.

Erkaev, N.V., Penz, T., Lammer, H., Lichtenegger, H.I.M., Wurz, P., Biernat, H.K., Grießmeier, J.-M., Weiss, W.W., 2005. Plasma and magnetic field parameters in the vicinity of short periodic giant exoplanets. Astrophys. J. Suppl. Series 157, 396–401.

Gopalswamy, N., 2003. Coronal mass ejections: initiation and detection. Adv. Space Res. 31, 869–881.

Gopalswamy, N., 2004. A global picture of CMEs in the inner heliosphere. In: Poletto, G., Suess, S. (Eds.), The Sun and the Heliosphere as an Integrated System, ASSL Series. Kluwer Academic Publishers, pp. 201–240.

Gopalswamy, N., Kundu, M.R., 1993. Thermal and non-thermal emissions during a coronal mass ejection. Solar Phys. 143, 327–343.

Gopalswamy, N., Kaiser, M.L., Thompson, B.J., Burlaga, L.F., Szabo, A., Vourlidas, A., Lara, A., Yashiro, S., Bougeret, J.L., 2000. Radio-rich solar eruptive events. Geophys. Res. Lett. 27, 1427–1430.

Gopalswamy, N., Yashiro, S., Kaiser, M.L., Howard, R.A., Bougeret, J.-L., 2001a. Characteristics of coronal mass ejections associated with long-wavelength type II radio bursts. J. Geophys. Res. 106 (A12), 29219–29230.

Gopalswamy, N., Lara, A., Yashiro, S., Kaiser, M.L., Howard, R.A., 2001b. Predicting the 1-AU arrival times of coronal mass ejections. J. Geophys. Res. 106 (A12), 29207–29218.

Gopalswamy, N., Yashiro, S., Kaiser, M. L., Howard, R. A., Bougeret, J.-L., 2002. Interplanetary radio emission due to interaction between two coronal mass ejections. Geophys. Res. Lett. 29(8), doi:10.1029/2001GL013606.

Gopalswamy, N., Shimojo, M., Lu, W., Yashiro, S., Shibasaki, K., Howard, R.A., 2003a. Prominence eruptions and coronal mass ejection: a statistical study using microwave observations. Astrophys. J. 586, 562–578.

Gopalswamy, N., Lara, A., Yashiro, S., Howard, R.A., 2003b. Coronal mass ejections and solar polarity reversal. Astrophys. J. 598, L63–L66.

Grießmeier, J.-M., Stadelmann, A., Penz, T., Lammer, H., Selsis, F., Ribas, I., Guinan, E.F., Motschmann, U., Biernat, H.-K., Weiss, W.W., 2004. The effect of tidal locking on the magnetospheric and atmospheric evolution of "Hot Jupiters". Astron. Astrophys. 425, 753–762.

Guillot, T., Burrows, A., Hubbard, W.B., Lunine, J.I., Saumon, D., 1996. Giant planets at small orbital distances. Astrophys. J. 459, L35–L38.

Guinan, E.F., Ribas, I., 2002. Our changing Sun: the role of solar nuclear evolution and magnetic activity on Earth's atmosphere and climate. In: Montesinos, B., Giménz, A., Guinan, E.F. (Eds.), The Evolving Sun and Its Influence on Planetary Environments, vol. 269. ASP, San Francisco, pp. 85–107.

Henke, T., Woch, J., Mall, U., Livi, S., Wilken, B., Schwenn, R., Gloeckler, G., von Steiger, R., Forsyth, R.J., Balogh, A., 1998. Differences in the O7 + /O6+ ratio of magnetic cloud and non-cloud coronal mass ejections. Geophys. Res. Lett. 25, 3465–3468.

Hildner, E., Gosling, J.T., MacQueen, R.M., Munro, R.H., Poland, A.I., Ross, C.L., 1976. Frequency of coronal transients and solar activity. Solar Phys. 48, 127–135.

Howard, R.A., Michels, D., Sheeley, N.R., Koomen, M.J., 1986. The solar cycle dependence of coronal mass ejections. In: Marsden, R., Reidel, D. (Eds.), The Sun and the Heliosphere in Three Dimensions, vol. 123. ASSL, pp. 107–111.

Hundhausen, A.J., 1993. Sizes and locations of coronal mass ejections—SMM observations from 1980 and 1984–1989. J. Geophys. Res. 98, 13177–13200.

Kallio, E., Luhmann, J.G., Barabash, S., 1997. Charge exchange near Mars: the solar wind absorption and energetic neutral atom production. J. Geophys. Res. 102, 22183–22198.

Keppens, R., MacGregor, K.B., Charbonneau, P., 1995. On the evolution of rotational velocity distributions for solar-type stars. Astron. Astrophys. 294, 469–487.

Lammer, H., Selsis, F., Ribas, I., Guinan, E.F., Bauer, S.J., Weiss, W.W., 2003a. Atmospheric loss of exoplanets resulting from stellar X-ray and extreme ultraviolet heating. Astrophys. J. 598, L121–L124.

Lammer, H., Lichtenegger, H.I.M., Kolb, C., Ribas, I., Guinan, E.F., Abart, R., Bauer, S.J., 2003b. Loss of water from Mars: implications for the oxidation of the soil. Icarus 106, 9–25.

Langmayr, D., Erkaev, N.V., Penz, T., Lammer, H., Kulikov, Yu. N., Biernat, H. K., Selsis, F., Barge, P., Deleuil, M., Guis, V., Léger, A., 2006. Mass loss of "Hot Jupiters"—implications for CoRoT discoveries. Part II: long time thermal atmospheric evaporation modelling. Planet. Space Sci., submitted for publication.

Lara, A., González-Esparza, J.A., Gopalswamy, N., 2004. Characteristics of coronal mass ejections in the near Sun interplanetary space. Geofís. Int. 43, 75–82.

Lecavelier-des-Etangs, A., Vidal-Madjar, A., McConnell, J.C., Hébrard, G., 2004. Atmospheric escape from hot Jupiters. Astron. Astrophys. 418, L1–L4.

Lepri, S.T., Zurbuchen, T.H., Fisk, L.A., Richardson, I.G., Cane, H.V., Gloeckler, G., 2001. Iron charge distribution as an identifier of interplanetary coronal mass ejections. J. Geophys. Res. 106, 29231–29238.

Lichtenegger, H.I.M., Dubinin, E.M., 1998. Model calculations of the planetary ion distribution in the Martian tail. Earth Planets Space 50, 445–452.

Lichtenegger, H.I.M., Schwingenschuh, K., Dubinin, E.M., Lundin, R., 1995. Particle simulation in the Martian magnetotail. J. Geophys. Res. 100, 21659–21667.

Lichtenegger, H. I. M., Lammer, H., Stumptner, W., 2002. Energetic neutral atoms at Mars: III. Flux and energy distributions of planetary energetic H atoms. J. Geophys. Res. 107 (A10), doi:10.1029/2001JA000322.

Lindsay, G.M., Luhmann, J.G., Russell, C.T., Gosling, J.T., 1999. Relationships between coronal mass ejection speeds from coronagraph images and interplanetary characteristics of associated interplanetary coronal mass ejections. J. Geophys. Res. 104, 12515–12524.

Luhmann, J.G., 1993. A model of the ionospheric tail rays of Venus. J. Geophys. Res. 98, 17615–17621.

Moutou, C., Brage, P., Deleuil, M., Jorda, L., the COROT Team, 2003. The CoRoT mission: status. In: Deming, D., Seager, S. (Eds.), Scientific Frontiers in Research on Extrasolar Planets. ADS Series, vol. 294, San Francisco, pp. 423–426.

Noyes, R.W., Hartmann, L.W., Baliunas, S.L., Duncan, D.K., Vaughan, A.H., 1984. Rotation, convection, and magnetic activity in lower main-sequence stars. Astrophys. J. 279, 763–777.

Pätzold, M., Rauer, H., 2002. Where are the massive close-in extrasolar planets? Astrophys. J. 568, L117–L120.

Penz, T., Erkaev, N.V., Biernat, H.K., Lammer, H., Amerstorfer, U.V., Gunell, H., Kallio, E., Barabash, S., Orsini, S., Milillo, A., Baumjohann, W., 2004. Ion loss on Mars caused by the Kelvin–Helmholtz instability. Planet. Space Sci. 52, 1157–1167.

Ribas, I., Guinan, E.F., Güdel, M., Audard, M., 2005. Evolution of the solar activity over time and effects on planetary atmospheres. I. High-energy irradiances (1–1700 Å). Astrophys. J. 622, 680–694.

Sánchez-Lavega, A., 2004. The magnetic field in giant extrasolar planets. Appl. Phys. J. 609, L87–L90.

Sheeley, N., Howard, R.A., Koomen, M.J., Michels, D.J., 1983. Associations between coronal mass ejections and soft X-ray events. Astrophys. J. 272, 349–354.

Simon, T., Boesgaard, E.F., Herbig, G., 1985. The evolution of chromospheric activity and the spin-down of solar-type stars. Appl. Phys. J. 293, 551–570.

Skumanich, A., 1972. Timescales for CA II emission decay, rotational braking and lithium depletion. Astrophys. J. 171, 565–567.

St. Cyr, O.C., Howard, R.A., Sheeley, N.R. Jr., Plunkett, S.P., Michels, D.J., Paswaters, S.E., Koomen, M.J., Simnett, G.M., Thompson, B.J., Gurman, J.B., Schwenn, R., Webb, D.F., Hildner, E., Lamy, P.L., 2000. Properties of coronal mass ejections: SOHO LASCO observations from January 1996 to June 1998. J. Geophys. Res. 105, 18169–18185.

Stadelmann, A., 2004. Globale Effekte einer Erdmagnetfeldumkehrung: Magnetosphärenstruktur und kosmische Teilchen. Ph.D. Thesis, Technische Universität Braunschweig, Braunschweig, Germany.

Tian, F., Toon, O.B., Pavlov, A.A., DeSterck, H., 2005. Transonic hydrodynamic escape of hydrogen from extrasolar planetary atmospheres. Astrophys. J. 621, 1049–1060.

Vidal-Madjar, A., Lecavelier des Etangs, A., Désert, J.-M., Ballester, G.E., Ferlet, R., Hébrard, G., Mayor, M., 2003. An extended upper atmosphere around the extrasolar planet HD209458b. Nature 422, 143–146.

Vidal-Madjar, A., Désert, J.-M., Lecavelier des Etangs, A., Hébrard, G., Ballester, G.E., Ehrenreich, D., Ferlet, R., McConnell, J.C., Mayor, M., Parkinson, C.D., 2004. Detection of oxygen and carbon in the hydrodynamically escaping atmosphere of the extrasolar planet HD209458b. Astrophys. J. 604, L69–L72.

Voigt, G.-H., 1981. A mathematical magnetospheric field model with independent physical parameters. Planet. Space Sci. 29, 1–20.

Vourlidas, A., Buzasi, D., Howard, R.A., Esfandiari, E., 2002. Mass and energy properties of LASCO CMEs. In: Wilson, A. (Ed.), Solar Variability: From Core to Outer Frontiers. ESA SP-506, Noordwijk, pp. 91–94.

Webb, D.F., Howard, R.A., 1994. The solar cycle variation of coronal mass ejections and the solar wind mass flux. J. Geophys. Res. 99, 4201–4220.

Wood, B.E., Müller, H.-R., Zank, G., Linsky, J.L., 2002. Measured mass loss rates of solar-like stars as a function of age and activity. Astrophys. J. 574, 412–425.

Wood, B.E., Müller, H.-R., Zank, G.P., Linsky, J.L., Redfield, S., 2005. New mass-loss measurements from astrospheric Ly-α absorption. Astrophys. J. 628, L143–L146.

Wright, J.T., Marcy, G.W., Butler, R.P., Vogt, S.S., 2004. Chromospheric Ca II emission in nearby F, G, K, and M stars. Astrophys. J. Suppl. Series 152, 261–295.

Wurz, P., Lammer, H., 2003. Monte-Carlo simulation of Mercury's exosphere. Icarus 164, 1–13.

Yashiro, S., Gopalswamy, N., Michalek, G., St. Cyr, O.C., Plunkett, S.P., Rich, N.B., Howard, R.A., 2004. A catalog of white light coronal mass ejections observed by the SOHO spacecraft. J. Geophys. Res. 109 (A7), doi:10.1029/2003JA010282.

Yelle, R., 2004. Aeronomy of extra-solar giant planets at small orbital distances. Icarus 170, 167–179.

Zahnle, K.J., Walker, J.C.G., 1982. The evolution of solar ultraviolet luminosity. Rev. Geophys. 20, 280–292.

Zhang, J., Dere, K.P., Howard, R.A., Kundu, M.R., White, S.M., 2001. On the temporal relationship between coronal mass ejections and flares. Astrophys. J. 559, 452–462.